THE JOURNAL OF PHYSICAL CHEMISTRY A

ARTICLE

pubs.acs.org/JPCA

Site-Specific Rate Coefficients for Reaction of OH with Ethanol from 298 to 900 K

Scott A. Carr, Mark A. Blitz, and Paul W. Seakins*

School of Chemistry, University of Leeds, Leeds, LS2 9JT, United Kingdom

ABSTRACT: The rate coefficients for reactions of OH with ethanol and partially deuterated ethanols have been measured by laser flash photolysis/laser-induced fluorescence over the temperature range 298−523 K and 5−100 Torr of helium bath gas. The rate coefficient, $k_{1.1}$, for reaction of OH with C_2H_5OH is given by the expression $k_{1.1} = 1.06 \times 10^{-22} T^{3.58} \exp(1126/T)$ cm^3 molecule^{-1} s^{-1}, and the values are in good agreement with previous literature. Site-specific rate coefficients were determined from the measured kinetic isotope effects. Over the temperature region 298−523 K abstraction from the hydroxyl site is a minor channel. The reaction is dominated by abstraction of the α hydrogens (92 ± 8)% at 298 K decreasing to (76 ± 9)% with the balance being abstraction at the β position where the errors are 2σ. At higher temperatures decomposition of the CH_2CH_2OH product from β abstraction complicates the kinetics. From 575 to 650 K, biexponential decays were observed, allowing estimates to be made for $k_{1.1}$ and the fractional production of CH_2CH_2OH. Above 650 K, decomposition of the CH_2CH_2OH product was fast on the time scale of the measured kinetics and removal of OH corresponds to reaction at the α and OH sites. The kinetics agree (within ±20%) with previous measurements. Evidence suggests that reaction at the OH site is significant at our higher temperatures: 47−53% at 865 K.

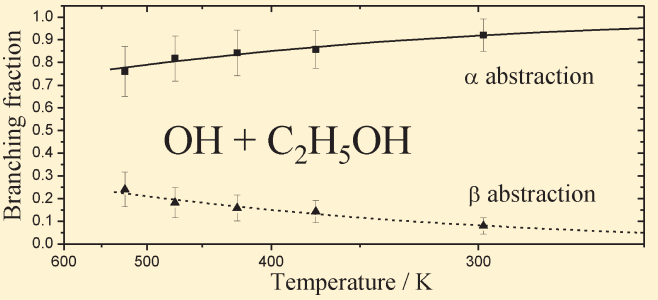

INTRODUCTION

Ethanol has many desirable qualities as a transportation fuel; it can be blended with gasoline and used in conventional spark ignition engines, it has a relatively high energy density and a high octane number, and its high oxygen ratio results in reduced tailpipe emissions of many regulated compounds such as carbon monoxide and aromatics. Ethanol has a lower toxicity than other oxygenates such as methanol or methyl tertiary butyl ether (MTBE). Much of the current interest stems from the environmental and energy security advantages of generating ethanol from biomass.[1]

While ethanol has many advantages as a fuel, enhanced use of ethanol will result in increased release of ethanol (unburnt fuel, fugitive emissions, and emissions during production) and acetaldehyde and formaldehyde from the combustion process. The atmospheric oxidation of ethanol leads to important secondary pollutants such as acetaldehyde, peroxyacetylnitrate (PAN), formaldehyde, and ozone.

Under atmospheric and low-temperature combustion conditions (<∼1100 K) the abstraction reaction R1 with the hydroxyl radical, OH, is the major ethanol consumption process

$$OH + CH_3CH_2OH \rightarrow H_2O + C_2H_5O \quad (R1)$$

Abstraction can occur at three sites leading to different C_2H_5O isomers which subsequently react to give different first-generation stable products

$$OH + CH_3CH_2OH \rightarrow H_2O + CH_3CHOH \quad \alpha \text{ abstraction} \quad (R1a)$$

$$OH + CH_3CH_2OH \rightarrow H_2O + CH_3CH_2OH \quad \beta \text{ abstraction} \quad (R1b)$$

$$OH + CH_3CH_2OH \rightarrow H_2O + CH_3CH_2O \quad \text{hydroxyl abstraction} \quad (R1c)$$

In the atmosphere the CH_3CHOH (α-hydroxyethyl) and CH_3CH_2O (ethoxy) radicals will react with molecular oxygen, leading to production of acetaldehyde and HO_2 (reactions R2 and R3), whereas the CH_2CH_2OH (β-hydroxyethyl) radical reacts primarily via O_2 addition to form a peroxy radical. In the polluted or semipolluted atmosphere subsequent reaction with NO and alkoxy radical decomposition leads to production of two molecules of formaldehyde via reactions R4a−R7.

$$CH_3CHOH + O_2 \rightarrow CH_3CHO + HO_2 \quad (R2)$$

$$CH_3CH_2OH + O_2 \rightarrow CH_3CHO + HO_2 \quad (R3)$$

$$CH_2CH_2OH + O_2 + M \rightarrow OOCH_2CH_2OH + M \quad (R4a)$$

Received: January 7, 2011
Revised: March 11, 2011
Published: March 28, 2011

$$OOCH_2CH_2OH + NO \rightarrow OCH_2CH_2OH + NO_2 \quad (R5)$$

$$OCH_2CH_2OH \rightarrow HCHO + CH_2OH \quad (R6)$$

$$CH_2OH + O_2 \rightarrow HCHO + HO_2 \quad (R7)$$

At high temperatures CH_2CH_2OH can decompose to regenerate OH, reaction R8a, and at low pressures the chemically activated peroxy radical formed following O_2 addition can undergo rearrangements including a channel R4b to regenerate OH[2−4]

$$CH_2CH_2OH \rightarrow C_2H_4 + OH \quad (R8a)$$

$$CH_2CH_2OH \rightarrow \text{non-OH product channels} \quad (R8b)$$

$$CH_2CH_2OH + O_2 \rightarrow OOCH_2CH_2OH^* \rightarrow OH + 2HCHO \quad (R4b)$$

Additionally, at high temperatures the ethoxy radical can decompose to yield methyl radicals and formaldehyde

$$CH_3CH_2O \rightarrow CH_3 + HCHO \quad (R9)$$

The overall rate coefficient for reaction R1 is well characterized. IUPAC[5] recommends $k_1 = 6.70 \times 10^{-18}\ T^2 \exp(511/T)$ cm^3 molecule^{-1} s^{-1} over the temperature range 216−599 K based on the studies of Hess and Tully,[6] Wallington and Kurylo,[7] Jimenez et al.,[8] and Dillon et al.[9] with a 298 K value of 3.2×10^{-12} cm^3 molecule^{-1} s^{-1} ($\Delta \log k = 0.08$). However, uncertainty in the branching ratios, Φ, for reaction R1 is much greater. IUPAC recommends Φ_{1a} (k_{1a}/k_1) = 0.9 at 298 K and $\Phi_{1b} = \Phi_{1c} = 0.05$ primarily based on the kinetic data of Hess and Tully using isotopically labeled OH.[6,10] The value of $\Phi_{1a} = 0.9$ is consistent with a mass spectrometric study by Meier et al.,[11] who determined $\Phi_{1a} = 0.75 \pm 0.15$ at 298 K. Little is known about the temperature dependence of the branching ratios; however, given the greater bond strengths of the β C−H and O−H bonds in ethanol, one would expect channels Φ_{1b} and Φ_{1c} to become more significant at higher temperature.

A wide variety of different branching ratios for reaction R1 have been used in modeling studies of low-temperature ethanol combustion. Frassoldati et al.[12] reviewed different models; the branching ratio Φ_{1a} at 900 K ranges from ∼0.8[13] to 0.25.[14] Frassoldati et al. noted that models of flame speeds in laminar burning experiments were highly sensitive to the branching ratios Φ_{1a} and Φ_{1b}. Given the uncertainty in branching ratios for reaction R1 there is a clear need for additional experimental data.

In this study the branching ratios Φ_{1a}, Φ_{1b}, and Φ_{1c} have been determined from 298 to 523 K by studying the kinetics of isotopically labeled ethanol in a similar manner to the work of Dunlop and Tully.[15] The following reactions were studied, monitoring removal of OH radicals by laser-induced fluorescence (LIF) under pseudo-first-order conditions after photolytic generation of OH

$$OH + CH_3CH_2OH \rightarrow \text{products} \quad (R1.1)$$

$$OH + CD_3CH_2OH \rightarrow \text{products} \quad (R1.2)$$

$$OH + CH_3CD_2OH \rightarrow \text{products} \quad (R1.3)$$

$$OH + CD_3CD_2OH \rightarrow \text{products} \quad (R1.4)$$

$$OH + CH_3CH_2OD \rightarrow \text{products} \quad (R1.5)$$

$$OH + CD_3CD_2OD \rightarrow \text{products} \quad (R1.6)$$

Assuming that the rate coefficient is independent of the isotopic content at other sites in the molecule, then the rate coefficients for reactions R1.1−R1.6 can be written in terms of the site-specific rate coefficients and kinetic isotope effects (KIE).

Above 550 K decomposition of the CH_2CH_2OH radical to regenerate OH produces biexponential OH traces, complicating the analysis, but branching ratio information can still be retrieved. Potential effects from OH recycling via reactions R4b and R8a are also investigated at temperatures below 600 K. At temperatures above 650 K decomposition of CH_2CH_2OH becomes rapid on the time scale of the kinetics and OH traces once again become simple exponentials; however, assuming that reaction R4b is the only loss process for CH_2CH_2OH, the OH decays now yield the rate coefficients for loss via channels R1a and R1c. Very recently Sivaramakrishnan et al.[16] carried out a study of reaction R1 over the temperature range 857−1297 K using shock tube methods. As they too monitor OH loss, the rate coefficient that they report, $k = (2.5 \pm 0.4) \times 10^{-11} \exp(-(911 \pm 191)\ K/T)$ cm^3 molecule^{-1} s^{-1}, is for channels R1a and R1c (assuming that all CH_2CH_2OH decomposes to regenerate OH). Sivaramakrishnan et al. complemented their experimental measurements with ab initio (QCISD(T)/CBS)/TST calculations of site-specific rate coefficients. Other theoretical calculations have been performed by Xu and Lin[17] (CCSD(T)/6-311+G(3df,2p)//MP2/6-311+G(3df,2p) and Galano et al.[18] (CCSD(T)/6-311G(d,p)//BHand HLYP/6-311G). In the final section of the paper we compare our results with various theoretical and modeling studies.

EXPERIMENTAL SECTION

All experiments were carried out in a metal slow flow flash photolysis apparatus as described in previous publications.[19−21] The OH precursor, ethanol, and helium bath gas were flowed through calibrated flow controllers into a mixing manifold and hence into the reaction cell. The total pressure in the cell was controlled by a throttle between the cell and the rotary pump. Pressures in the cell were measured using a baratron pressure gauge. The cell was a six-way cross constructed from stainless steel, the central portion could be heated with cartridge heaters (Watlow), and the temperature above and below the reaction region was monitored with thermocouples which provided a feedback signal to the heater control.

OH radicals were generated by pulsed laser photolysis (Lambda Physik, Compex, KrF at 248 nm or ArF at 193 nm) of a precursor and monitored via off-resonance laser-induced fluorescence (LIF). The probe laser light, introduced into the cell perpendicularly to the photolysis laser beam, was the frequency-doubled output of a pulsed NdYAG (Spectra-Physics, Quanta-Ray GCR 100-series) pumped dye laser (Spectra-Physics, Quanta-Ray PDL-3) operating with Rhodamine 6G dye. This was tuned to the energy of the OH ($A^2\Sigma(v = 1) \leftarrow X^2\Pi(v = 0)$, $Q_1(1)$) transition at ∼281.9 nm. Fluorescence was detected through a 308 nm filter by a photomultiplier tube mounted on top of the reaction cell, perpendicular to the plane of the photolysis and probe laser beams. The signal was averaged on a boxcar integrator before being transferred to a PC for analysis.

Table 1. Bimolecular Rate Coefficients for Reaction of OH with Various Deuterated Forms of Ethanol[a]

	$k/10^{-12}$ cm^3 molecule^{-1} s^{-1}			
T/K	CH_3CH_2OH	CD_3CH_2OH	CH_3CH_2OD	fraction of ROD
298	3.26 ± 0.08[b]	2.98 ± 0.07	3.32 ± 0.08	0.72−0.83
298	3.36 ± 0.09[c]			
298	3.29 ± 0.09[d]			
373	3.72 ± 0.09	3.29 ± 0.09	3.73 ± 0.10	0.75
423	3.87 ± 0.13	3.53 ± 0.09	3.87 ± 0.10	0.89
473	4.32 ± 0.11	3.75 ± 0.10	4.33 ± 0.11	0.85
523	4.57 ± 0.12	4.35 ± 0.14	4.52 ± 0.12	0.89
523	4.76 ± 0.13[c]			
523	4.87 ± 0.17[d]			
T/K	CD_3CD_2OH	CH_3CD_2OH	CD_3CD_2OD	fraction of ROD
298	1.42 ± 0.04	1.62 ± 0.04	1.40 ± 0.03	0.83
298		1.67 ± 0.07[c]		
373	1.87 ± 0.05	2.25 ± 0.06	1.77 ± 0.05	0.78
423	2.15 ± 0.05	2.55 ± 0.06	2.28 ± 0.06	0.79
473	2.60 ± 0.07	3.08 ± 0.08	2.49 ± 0.06	0.85
523	2.87 ± 0.08	3.51 ± 0.09	2.75 ± 0.07	0.84
523		3.48 ± 0.12[c]		
523		3.79 ± 0.13[d]		

[a] For reactions R1.5 and R1.6 the fraction of exchange ([ROD]/([ROD + ROH]) was measured using FTIR, see text. [b] Average of six repeat measurements. [c] N_2O/H_2O precursor, pressure = 5 Torr, $[O_2] > 1 \times 10^{16}$ molecules cm^{-3}. [d] N_2O/H_2O precursor, pressure = 5 Torr, zero O_2. Errors are 2σ.

Three OH precursors were used to generate OH in either a dry environment to minimize exchange reactions of the deuterated ethanols CH_3CH_2OD and CD_3CD_2OD or an O_2-free environment. The dry OH source was 248 nm photolysis of acetone and the subsequent reaction of CH_3CO radicals with O_2.[19]

$$CH_3COCH_3 + h\nu \rightarrow CH_3CO + CH_3 \quad (R10)$$

$$CH_3CO + O_2 \rightarrow OH + \text{products} \quad (R11)$$

The O_2 free experiments were performed using 193 nm photolysis of N_2O in the presence of H_2O

$$N_2O + h\nu \rightarrow O(^1D) + N_2 \quad (R12)$$

$$O(^1D) + H_2O \rightarrow 2HO \quad (R13)$$

or the 248 nm photolysis of t-butyl hydroperoxide (TBH).

$$(CH_3)_3COOH + h\nu \rightarrow (CH_3)_3CO + OH \quad (R14)$$

Reaction R13 produces vibrationally excited OH;[22] however, this is efficiently relaxed by water, generating ground state OH on time scales of a few microseconds or less, and could be treated as an instantaneous source when measuring millisecond OH decay profiles.

CH_3CH_2OH (Aldrich, ≥99.5% (200 proof), CD_3CH_2OH (Aldrich, 99 atom % D),CH_3CD_2OH (Aldrich, 99 atom % D), CH_3CH_2OD (Aldrich, 99.5 atom % D), CD_3CD_2OH (Aldrich, 99.5 atom % D),CD_3CD_2OD (Aldrich, 99.5 atom % D), *tert*-butyl hydroperoxide (70% aq), and acetone (99%+) were purified by several freeze−pump−thaw cycles. He (BOC, CP grade, 99.999%), O_2 (Air Products, high purity, 99.999%), and N_2O (Fluka, >99.998%) were used without further purification.

A particular problem when flowing alcohols deuterated at the hydroxyl group (CH_2CH_2OD or CD_3CD_2OD, referred to as ROD) was for proton exchange, ROD → ROH, to occur before the alcohol samples passed through the photolysis region of the reaction cell. To measure the amount of exchange occurring in this work, FTIR (Nicolet Avatar 360 E.S.P.) analysis of the reaction mixture was undertaken by taking samples using a liquid nitrogen trap placed in the exhaust line of the reaction cell. The amount of exchange was substantially reduced by using the acetone/O_2 precursor, which is a dry OH source that does not contain a hydroxyl functional group. The cause of the remaining exchange was possibly atmospheric water adsorbed on the surface of the stainless steel vacuum line and reaction cell, and although attempts were made to remove the effect there was always some small fraction of exchange present during the experiment. Therefore, the fraction of exchange was quantified by FTIR analysis for each set of kinetic measurements, giving [ROD]/([ROD] + [ROH]) = 0.72−0.89, see Table 1. Exchange occurring during the trapping process could not be ruled out, so the fraction presented represents an upper limit to the actual fraction of exchange in the cell. Analysis of the gas mixture when CD_3CD_2OH was present had no detectable C−H peak, confirming the isotopic purity of the alcohol and that exchange at the α and β sites was not occurring. This was also confirmed for the other deuterated ROH alcohols, as the relative heights of the C−H and C−D peaks did not change before and after passing through the reaction cell.

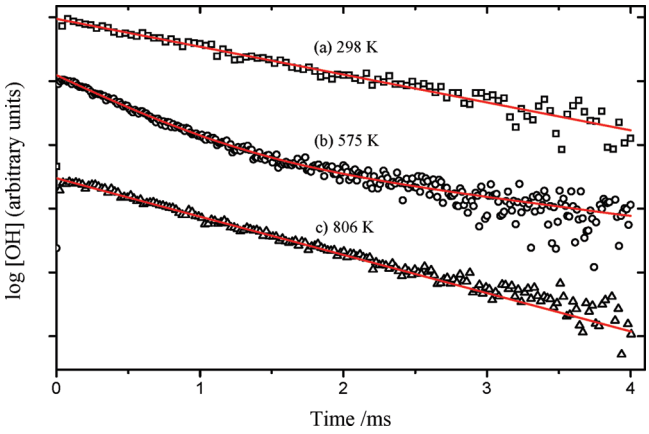

Figure 1. Fluorescence signal vs time following 193 nm photolysis of mixtures of $N_2O/H_2O/CH_3CH_2OH$/He at three different temperatures: (a) T = 298 K, $[CH_3CH_2OH] = 4.3 \times 10^{14}$ molecules cm^{-3}, $[N_2O] = 1.1 \times 10^{16}$ molecules cm^{-3}, $[OH]_0 \approx 1.4 \times 10^{11}$ molecules cm^{-3}; (b) T = 575 K, $[CH_3CH_2OH] = 0.96 \times 10^{14}$ molecules cm^{-3}, $[N_2O] = 5.8 \times 10^{15}$ molecules cm^{-3}, $[OH]_0 \approx 1.3 \times 10^{11}$ molecules cm^{-3}; (c) T = 806 K, $[CH_3CH_2OH] = 0.5 \times 10^{14}$ molecules cm^{-3}, $[N_2O] = 3.7 \times 10^{15}$ molecules cm^{-3}, $[OH]_0 \approx 0.6 \times 10^{11}$ molecules cm^{-3}. The y axis is in decades, with traces off set for clarity.

RESULTS

Figure 1 shows examples of typical log plots of the OH signal in the presence of excess ethanol as a function of time for three different temperature regimes.

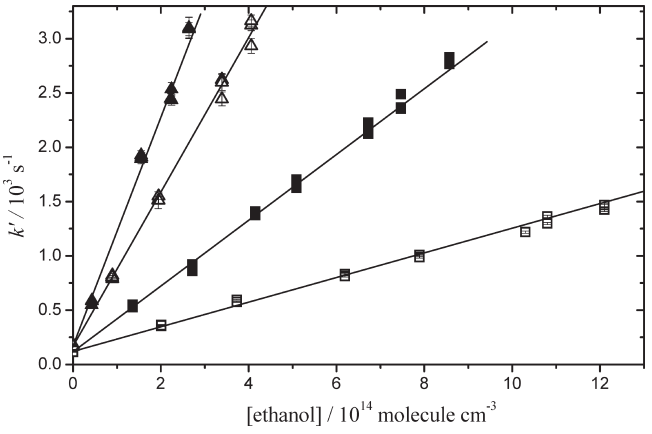

Figure 2. Bimolecular plot showing k' versus [ethanol]: filled shapes, CH_3CH_2OH; empty shapes, CD_3CD_2OH; squares, 298 K; triangles, 806 K.

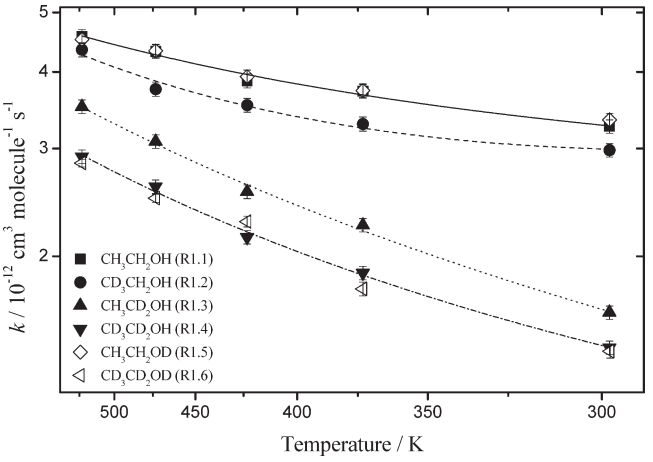

Figure 3. Bimolecular rate coefficients for reactions of OH with various deuterated isotopomers of ethanol (298 K < T < 573 K): CH_3CH_2OH, filled squares; CD_3CH_2OH, filled circles; CH_3CD_2OH, filled upward triangles; CD_3CD_2OH, filled downward triangles; CH_3CH_2OD, empty squares; CD_3CD_2OD, empty triangles. Error bars are statistical uncertainties at the 2σ level obtained from fitting to the bimolecular plots.

Below 523 K, [OH] removal was governed by reaction R1 only and so under pseudo-first-order conditions a linear log[OH] vs time trace was observed. Between 550 and 650 K, biexponential kinetic traces were observed due to OH recycling from decomposition of the CH_2CH_2OH radical, reaction R8a.[6] Above 650 K, k_8 was fast compared with the pseudo-first-order OH loss rate coefficient and so the [OH] kinetic profiles were again characterized by single-exponential loss. The observed OH loss rate was slower than the total rate of OH consumed by reaction R1 by a factor equal to the yield of OH recycled through reactions R1b and R8a.

With acetone/O_2 as the OH precursor typical concentrations were [alcohol] = 0.5−10 × 10^{14} molecules cm^{-3}, [acetone] = 5 × 10^{13} molecules cm^{-3}, [O_2] = 1−5 × 10^{16} molecules cm^{-3}, and He buffer gas 25 Torr. The photolysis laser powers used varied between 10 and 20 mJ $pulse^{-1}$, corresponding to photon densities of approximately 5−10 × 10^{15} photon cm^{-2} s^{-1}. An upper limit of the initial OH concentration ($[OH]_0$) was estimated to be 0.5−1.5 × 10^{11} molecules cm^{-3}, assuming a quantum yield of unity and the recommended absorption cross section for acetone.[23] The condition [alcohol]/$[radicals]_0$ > 500 was maintained in almost all experiments, ensuring OH concentrations followed pseudo-first-order kinetics. Additionally, the ratio $k_{11}[O_2]/k_{1.1-1.6}$[alcohol] was maintained such that production of OH growth could be treated as instant and below 523 K OH loss could be considered as a simple exponential decay. A least-squares regression fit to the fluorescence signal, $I_{f,OH}$, time dependence was performed using equation E1

$$I_{f,OH}(t) = I_{f,OH}(0)\exp(-k't) \qquad \text{(E1)}$$

where $k' = k_{1.1-1.6}$ [alcohol] + k_{loss} was the pseudo-first-order rate coefficient, $k_{1.1-1.6}$ represents the bimolecular rate coefficients for reactions R1.1−R1.6, and k_{loss} represents the sum of first-order loss processes for OH due to diffusion and reaction with precursor and impurities. The assumption that k_{loss} followed first-order loss was reasonable as the observed traces when [alcohol] = 0 conformed to single-exponential behavior at all temperatures. To obtain bimolecular rate coefficients, values of k' were measured at different alcohol concentrations for a fixed precursor concentration. The gradient of a linear least-squares fit to a plot of k' vs [alcohol] gave the bimolecular rate coefficient. Typical bimolecular plots are shown in Figure 2 for reaction of OH + CH_3CH_2OH and OH + CH_3CD_2OH at 298 and 806 K.

After changing the alcohol flow rate, reproducible kinetics were only obtained after allowing several minutes for adsorption of the alcohol onto the walls of the reaction cell and gas line to reach equilibrium. Table 1 lists the rate coefficients for reactions of OH with the isotopomers of ethanol, $k_{1.1-1.6}$, which are plotted in Arrhenius form in Figure 3. The 2σ values obtained from the linear fit were typically ∼1−2%, see Table 1. However, these do not account for uncertainties that arise from sample preparation and calibration of the gas flow, pressure, and temperature in the cell. An estimate of the total random error was obtained from repeat measurements of the room temperature rate coefficient, obtained each time a sample was prepared. The error of six repeat readings of $k_{1.1}$ at room temperature, after weighting with the t-student value for five degrees of freedom for 95% confidence interval, was 4%. Combining this uncertainty with the precision gives an estimate of the smallest reliable KIEs observable in the system to be 5%.

Product branching ratios were obtained based on the methodology of Dunlop and Tully.[15] Such an approach requires accurate and precise rate coefficient measurements. The dry acetone/O_2 OH precursor[19] minimized the exchange process at the OH group but opened up the possibility of OH recycling from the reaction of CH_2CH_2OH with O_2, reaction R4b. The invariance of the measured rate coefficient for reaction R1.1 with precursor suggests that recycling is not significant under our experimental conditions. However, during the course of this study Zador et al.[4] reported a high yield of formaldehyde from reaction R4b, suggesting that this recycling could be significant even at low temperatures. We therefore undertook an analysis of OH recycling in the presence of oxygen.

Reaction R4b was studied by generation of $HOCH_2CH_2$ (from the OH + C_2H_4 reaction) in the presence of low concentrations of O_2 so that regeneration occurs on comparable time scales to OH removal. The resultant biexponential decays can be analyzed to determine recycling. Alternatively, we compared the rate coefficients for OH + C_2H_4 in the presence/absence

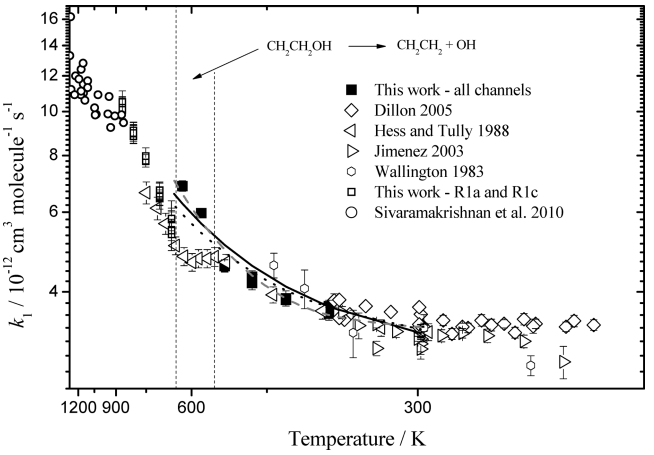

Figure 4. Arrhenius plot of the kinetic data obtained for reaction R1.1 in this study and in previous literature. Solid squares are the total rate coefficient for reaction R1.1. Empty squares are reduced by the rate of recycling OH. Error bars are the quoted 2σ values. Lines are fits of eqs E5 (black solid, $AT^2\exp(B/T)$ fit to our data), E6 (dotted line, $AT^2\exp(B/T)$ from IUPAC), and E7 (dashed line, $AT^n\exp(B/T)$ fit to our data).

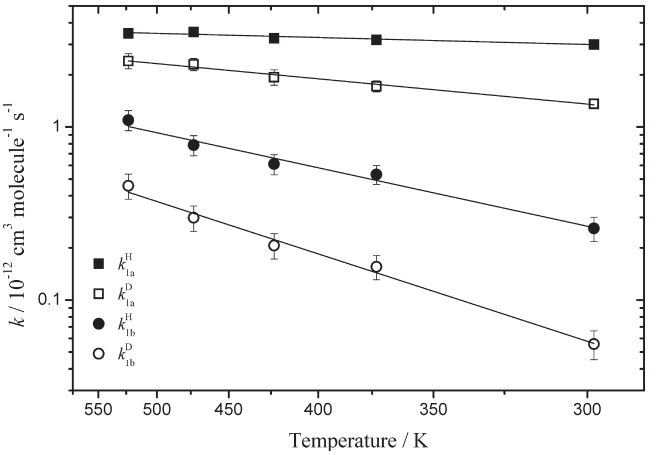

Figure 5. Site-specific rate coefficients for reaction R1 obtained from solving eq E3.

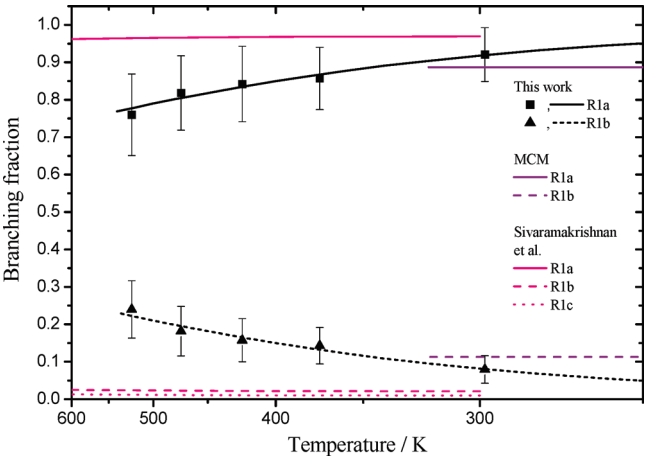

Figure 6. Branching fractions for reaction of OH + ethanol as a function of temperature: black triangles, Φ_{1b} from this work; black squares, Φ_{1a} from this work; filled lines, Φ_{1a}; dashed lines, Φ_{1b}; dotted lines, Φ_{1c}; black lines, this work; purple lines, Master Chemical Mechanism;[32] pink lines, Sivaramakrishnan et al.[16] Errors bars show the propagated 2σ level errors.

of an excess of O_2. In this case regeneration of OH is fast and the decays are exponential. The results confirm OH recycling at low temperatures (298−423 K) and low pressures; however, OH recycling becomes insignificant above ∼25 Torr at the temperatures studied, in agreement with the invariance of our measured $k_{1.1}$ with OH precursor.

Comparison with Literature Data for the Rate Coefficient, $k_{1.1}$, of the Reaction OH + CH_3CH_2OH. The temperature dependence of $k_{1.1}$ (OH + CH_3CH_2OH) is shown in Arrhenius form in Figure 4, including results from previous studies. The values of $k_{1.1}$ are in excellent agreement with the temperature-dependent study of Hess and Tully[6] and the more recent determinations of Dillon et al.[9] and Jiménez et al.[8] The strong curvature is consistent with a change in mechanism at higher temperatures. Around room temperature, reaction R1a is expected to dominate due to the low barrier height (−0.4[16] and 1.7 kJ mol^{-1} [18]) to form CH_3CHOH, which is consistent with the weak temperature dependence in this region. At much lower temperatures formation of a prereaction complex, as seen in other reactions of OH with oxygenated species,[24,25] could lead to an increase in the rate coefficient. Above 298 K, the contributions of reactions R1b and R1c are expected to increase due to their larger barriers (R1b 5.5[16] and 10.8 kJ mol^{-1} [18] and R1c 15.5[16] and 12.42 kJ mol^{-1} [18]), consistent with the increased rate coefficient seen and the experimental activation energy below 523 K.

Product Branching Ratios in Reaction R1 from 298 to 523 K. From Figure 3 and Table 1 it can be seen by comparing $k_{1.1}/k_{1.5}$ and $k_{1.4}/k_{1.6}$ that, even allowing for some atom exchange (<30%), deuteration of the hydroxyl group produces no measurable kinetic isotope effect (KIE). A significant KIE is expected for abstraction at the hydroxyl site, and therefore, it is concluded that abstraction at the hydroxyl site is not significant below 523 K. This observation is in good agreement with the recent calculations of Xu and Lin[17] and Sivaramakrishnan et al.,[16] who both estimate Φ_{1c} to be ∼3% at 500 K.

To obtain product branching ratios at the α site (Φ_{1a}) and β site (Φ_{1b}) from the measured rate constants, $k_{1.1}-k_{1.4}$, the same approach as Dunlop and Tully[15] was used. This method relies on some assumptions about the kinetic isotope effects. First, the rate of abstraction at a hydrogen/deuterium site is assumed independent of the isotopic content at other sites in the compound. This was justified experimentally by Tully and co-workers[26−29] for hydrocarbons and alcohols and theoretically by Hu et al.[30] The rate of reactions R1.1−R1.6 can be written in terms of the site-specific rate coefficients and kinetic isotope effects (KIE) $z_{1a\text{-}c}$, where $z^{-1}{}_{1a}(T) = k^{D}{}_{1a}/k^{H}{}_{1a}$, $z^{-1}{}_{1b}(T) = k^{D}{}_{1b}/k^{H}{}_{1b}$, and $z^{-1}{}_{1c}(T) = k^{D}{}_{1c}/k^{H}{}_{1c}$

$$\begin{pmatrix} 1 & 1 & 1 \\ z_{1a}^{-1} & 1 & 1 \\ 1 & z_{1b}^{-1} & 1 \\ z_{1a}^{-1} & z_{1b}^{-1} & 1 \\ 1 & 1 & z_{1c}^{-1} \\ z_{1a}^{-1} & z_{1b}^{-1} & z_{1c}^{-1} \end{pmatrix} \begin{pmatrix} k_{1a} \\ k_{1b} \\ k_{1c} \end{pmatrix} = \begin{pmatrix} k_{1.1} \\ k_{1.2} \\ k_{1.3} \\ k_{1.4} \\ k_{1.5} \\ k_{1.6} \end{pmatrix} \quad \text{(E2)}$$

dx.doi.org/10.1021/jp200186t | J. Phys. Chem. A 2011, 115, 3335–3345

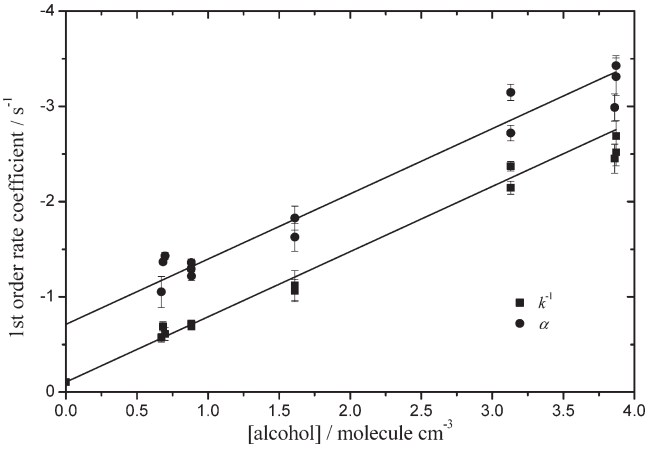

Figure 7. α parameter and k' versus $[CH_3CH_2OH]$ at 625 K and 25 Torr. Error bars are the returned 1σ values.

As no KIE is evident from reactions R1.5 and R1.6 these cannot be used in a quantitative analysis other than the assignment of $\Phi_{1c} = 0$, as discussed above, and eq E2 reduces to eq E3.

$$\begin{pmatrix} 1 & 1 \\ z_{1a}^{-1} & 1 \\ 1 & z_{1b}^{-1} \\ z_{1a}^{-1} & z_{1b}^{-1} \end{pmatrix} \begin{pmatrix} k_{1a} \\ k_{1b} \end{pmatrix} = \begin{pmatrix} k_{1.1} \\ k_{1.2} \\ k_{1.3} \\ k_{1.4} \end{pmatrix} \quad \text{(E3)}$$

The separation into site-specific branching ratios can be validated by comparing the magnitude of $k_{1.1} + k_{1.4}$ with $k_{1.2} + k_{1.3}$ (multiplying out the matrix equations, these both sum to $k_{1a}^{H} + k_{1b}^{H} + k_{1a}^{D} + k_{1b}^{D}$), which yield the same value within the errors, except for one datum at 523 K, Table 1. The system of equations is then reduced to four unknown parameters (k_{1a}, k_{1b}, z_{1a}, z_{1b}) but only three linearly independent equations. To reduce the dimensionality, Tully and co-workers assumed the KIE for β abstraction, z_{1b}, in 2-propanol is, to a good approximation, that measured for ethane and neopentane, $z_{1b} = 0.961 \exp(467/T)$, and so the same assumption is made here for ethanol. $k_{1.1}$, $k_{1.2}$, and $k_{1.4}$ were used to solve eq E3 as this led to smaller error than using $k_{1.3}$. The results using reaction R1.3 instead of reaction R1.4 in the analysis are within error except at 523 K. The site-specific rate coefficients are shown in Figure 5. Errors bars show the propagated errors at the 2σ level.

The solid lines are Arrhenius parametrizations of the data.

A least-squares regression fit was made to the site-specific rates using a two-parameter Arrhenius expression. The returned parameters are given below where the errors represent 2σ.

$$k_{1a}^{H} = (4.27 \pm 0.40) \times 10^{-12} \exp((-106 \pm 32/T)\ \text{cm}^3\ \text{molecule}^{-1}\ \text{s}^{-1}$$

$$k_{1a}^{D} = (5.10 \pm 0.75) \times 10^{-12} \exp((-397 \pm 27)/T)\ \text{cm}^3\ \text{molecule}^{-1}\ \text{s}^{-1}$$

$$k_{1b}^{H} = (5.99 \pm 2.62) \times 10^{-12} \exp((-933 \pm 179/T)\ \text{cm}^3\ \text{molecule}^{-1}\ \text{s}^{-1}$$

$$k_{1b}^{D} = (6.38 \pm 3.41) \times 10^{-12} \exp((-1418 \pm 117)/T)\ \text{cm}^3\ \text{molecule}^{-1}\ \text{s}^{-1}$$

Table 2. Rate Coefficients for Reactions R1.1 and R8a and Φ_{1b} from 575 to 650 K (errors are 2σ)

T/K	pressure/ Torr	$10^{12}k_{1.1}$/cm^3 molecule^{-1} s^{-1}	k_{8a}/s^{-1}	Φ_{1b}
575	25.0	5.97 ± 0.09	272 ± 58	0.22 ± 0.30
625	25.1	6.85 ± 0.18	596 ± 90	0.12 ± 0.18
650	25.1	6.80 ± 0.40	1187 ± 117	0.08 ± 0.14

The product branching fractions were calculated from the site-specific rate coefficients using eq E3, shown as a function of temperature in Figure 6. The figure includes the branching fraction calculated at each temperature and also using the Arrhenius parametrizations given above. Also included in the figure are the branching fraction for the atmospherically important β channel currently used in the Master Chemical Mechanism[31] and the theoretical calculations of Sivaramakrishnan et al.[16]

At 300 K the measured value of $\Phi_{1b} = 8\%$ is in good agreement with the current recommended IUPAC value of 5%. Extrapolations suggest that Φ_{1b} decreases to ~5% at temperatures of 220−230 K representative of the upper troposphere. Our results appear to validate the recent findings of Xu and Lin[17] and Sivaramakrishnan et al.[16] that Φ_{1c} is a minor channel below 523 K. However, the agreement between this work and the theoretical calculations is less consistent for Φ_{1b}; our values are slightly higher than those of Xu and Lin but significantly higher than Sivaramakrishnan et al. where Φ_{1b} is less than 4% at 500 K. Further comparisons of branching ratios from this work and literature values can be found below.

As the magnitudes of our yields depend strongly on the assumed values for z_{1b}, it is sensible to consider the effect of adjusting this value. As the C−H bonds in the methyl group in ethanol are weaker than those in hydrocarbons by a few kJ mol^{-1} a reduction in the exponent of z_{1b} might be reasonable. To give an indication of the possible effect, halving the exponent in z_{1b} increases the branching fraction by approximately a factor of 2, making the beta channel more significant. However, as discussed in the next section, direct values for Φ_{1b} could be obtained at higher temperatures, which confirm the branching fraction for reaction R1b is small.

Analysis of Kinetic Data from 575 to 650 K. From 575 to 650 K, the OH decays were biexponential in nature (Figure 1b) due to thermal decomposition of CH_2CH_2OH, reaction R8a

$$CH_2CH_2OH \rightarrow C_2H_4 + OH \quad \text{(R8a)}$$

Thermal decomposition of CH_3CO limited the high-temperature application of the acetone/O_2 OH source. Therefore, above 525 K, OH was generated only from 193 nm photolysis of N_2O and the subsequent reaction $O(^1D) + H_2O$. Assuming prompt OH formation from reactions R12 and R13, the OH concentration is governed by reactions R1 and R8a and other loss processes for CH_2CH_2OH (diffusion or other possible decomposition reactions, see below) represented as reaction R8b

$$CH_2CH_2OH \rightarrow \text{products other than OH} \quad \text{(R8b)}$$

Solution of the corresponding rate equations gives expression E4, which was fit to the experimental data to obtain parameters for $[OH]_0$, λ_+, λ_-, and k' for various concentrations of ethanol

$$[OH]_t = \frac{[OH]_0}{\lambda_+ - \lambda_-}[(k' - \lambda_-)\exp(-\lambda_+ t) - (k' - \lambda_+)\exp(-\lambda_- t)] \quad \text{(E4)}$$

dx.doi.org/10.1021/jp200186t |J. Phys. Chem. A 2011, 115, 3335–3345

Table 3. Apparent Rate Coefficients $\kappa_{1.1-1.4}$ between 658 and 864 K[a]

T/K	$\kappa_{1.1}/10^{-12}$ cm^3 molecule^{-1} s^{-1} (OH + CH_3CH_2OH)	$\kappa_{1.2}/10^{-12}$ cm^3 molecule^{-1} s^{-1} (OH + CD_3CH_2OH)	$\kappa_{1.3}/10^{-12}$ cm^3 molecule^{-1} s^{-1} (OH + CH_3CD_2OH)	$\kappa_{1.4}/10^{-12}$ cm^3 molecule^{-1} s^{-1} (OH + CD_3CD_2OH)
658	5.81 ± 0.23	5.64 ± 0.21		
698	6.43 ± 0.21	6.64 ± 0.22		
807	9.08 ± 0.29	9.20 ± 0.30		
864	10.30 ± 0.40	9.69 ± 0.37		
658	5.78 ± 0.23		3.79 ± 0.13	
698	6.68 ± 0.28		4.83 ± 0.17	
752	7.79 ± 0.25		5.60 ± 0.18	
807	9.07 ± 0.40		6.50 ± 0.21	
864	10.27 ± 0.36		7.82 ± 0.26	
658	5.79 ± 0.33			3.76 ± 0.19
698	6.59 ± 0.21			4.34 ± 0.14
806	8.82 ± 0.31			6.17 ± 0.22
864	10.24 ± 0.57			7.16 ± 0.34

[a] Errors are a combination of 2σ from a linear fit of the bimolecular plot combined with a 5% uncertainty to account for errors in the concentration of the alcohol.

where $k' = -k_1[\text{alcohol}] - k_{\text{loss}}$, $\lambda_\pm = ((\alpha \pm (\alpha^2+4\beta)^{1/2})/2)$, $\alpha = k_{8a}+k_{8b}-k'$

$$\beta = k_{1b}k_{8a}[\text{alcohol}] + (k_{8a} + k_{8b})k'$$

To obtain fittings with satisfactory statistics, 400 datum points, each consisting of the average of four laser pulses, were needed for each kinetic trace. Individual rate coefficients for k_1 and k_8 were extracted by performing linear fits to plots of k', $\alpha = (\lambda_+ + \lambda_-)$, and $\beta = (\lambda_+ \times \lambda_-)$ versus [alcohol], e.g., Figure 7. Values of $k_{1.1}$, k_{8a}, and Φ_{1b} are presented in Table 2.

Combining our lower temperature (298−523 K) measurements of $k_{1.1}$ with the values obtained for the biexponential regions gives the following modified Arrhenius parameters from an unweighted fit ($k_{1.1} = AT^n \exp(-E/RT)$, where the data have been fitted both by constraining n to 2, eq E5, to compare with IUPAC evaluation, eq E6, and allowing n to float, eq E7

$$k_{1.1} = 7.57 \times 10^{-18} T^2 \exp\left(\frac{469}{T}\right) \text{ cm}^3 \text{ molecule}^{-1} \text{ s}^{-1} \quad \text{(E5)}$$

$$k_{1.1} = 6.70 \times 10^{-18} T^2 \exp\left(\frac{511}{T}\right) \text{ cm}^3 \text{ molecule}^{-1} \text{ s}^{-1} \quad \text{(E6)}$$

$$k_{1.1} = 1.06 \times 10^{-22} T^{3.58} \exp\left(\frac{1126}{T}\right) \text{ cm}^3 \text{ molecule}^{-1} \text{ s}^{-1} \quad \text{(E7)}$$

Equations E5−E7 are shown as the lines in Figure 4.

Values for k_{1b} were poorly determined (e.g., $\Phi_{1b,\ 625\ K} = 0.12 \pm 0.18$) but consistent with β abstraction still being a minor but significant channel. While our experiments do not constrain Φ_{1b} particularly well, the observation of biexponential decays in this study and by Hess and Tully[6] as well as the apparent decrease in the observed rate coefficient for OH removal at high temperatures

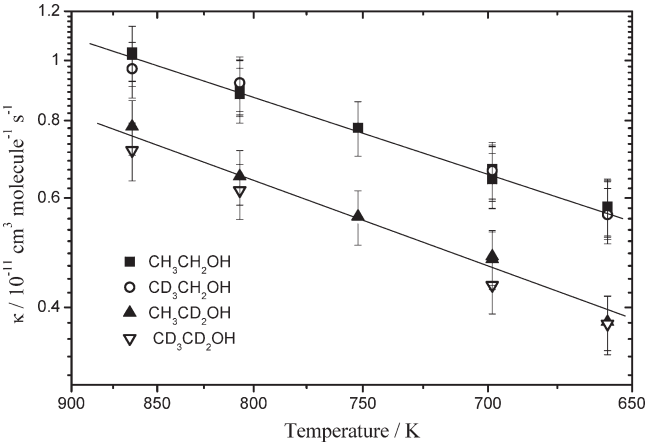

Figure 8. Bimolecular rate coefficients (658−864 K) for reactions of OH with several isotopomers of ethanol at 100 Torr.

(>650 K), compared to extrapolation of the 200−500 K data (Figure 4), shows that channel Φ_{1b} contributes to the reaction to a greater extent than that predicted by the calculations of Sivaramakrishnan et al.,[16] where Φ_{1b} is <4% up to 1000 K.

In their study of the OH + C_2H_4 ↔ $HOCH_2CH_2$ equilibrium, Diau and Lee[33] suggested that there was a significant additional chemical loss process for $HOCH_2CH_2$ other than reaction R8a accounting for approximately 25% of $HOCH_2CH_2$ removal. The presence of such a process would complicate the interpretation of the OH decays. However, the presence of an alternative decomposition or isomerization process was questioned in the experimental study of OH + C_2H_4 by Fulle et al.,[34] and recent high-level theoretical calculations by Senosiain et al.,[35] Cleary et al.,[21] and Xu et al.[36] appear to rule out alternative chemical loss processes for $HOCH_2CH_2$ below 650 K. The lack of an alternative decomposition channel for $HOCH_2CH_2$ is consistent with our experimental data; setting a value of k_{8b} above that expected from diffusion leads to negative values for Φ_{1b}.

Analysis of Kinetic Data from 700 to 864 K. Decomposition of the β-hydroxy radical is strongly temperature dependent and above 700 K OH is quickly recycled (k_8 > 2000 s^{-1}) following

dx.doi.org/10.1021/jp200186t |J. Phys. Chem. A 2011, 115, 3335–3345

Table 4. Returned Parameters from $AT^n \exp(-C/T)$ (weighted and unweighted) and $A\exp(-C/T)$ Fits to the Full Set of Kinetic Data

	weighted $AT^n \exp(-C/T)$	unweighted $AT^n \exp(-C/T)$	weighted $A\exp(-C/T)$
	$OH + CH_3CH_2OH \rightarrow H_2O + CH_3CHOH$		
A_{1aH}	$(2.54 \pm 0.05) \times 10^{-12}$ [a]	$(1.91 \pm 0.34) \times 10^{-12}$ [a]	$(3.8 \pm 1.2) \times 10^{-12}$ [a]
A_{1aD}	$(2.54 \pm 0.05) \times 10^{-12}$ [a,b]	$(1.91 \pm 0.34) \times 10^{-12}$ [a,b]	$(3.1 \pm 1.7) \times 10^{-12}$ [a]
C_{1aH}	-50.32 [c,d]	-50.32 [c,d]	72 ± 90 [c]
C_{1aD}	179.9 ± 7.4 [c]	277 ± 85 [c]	242 ± 139 [c]
n_{1a}	0.539 ± 0.082	1.19 ± 0.19	
	$OH + CH_3CH_2OH \rightarrow H_2O + CH_2CH_2OH$		
A_{1bH}	$(2.57 \pm 0.46) \times 10^{-12}$ [a]	$(4.2 \pm 3.7) \times 10^{-12}$	$(1.3 \pm 1.2) \times 10^{-11}$ [a]
A_{1bD}	$(2.57 \pm 0.46) \times 10^{-12}$ [a,b]	$(4.2 \pm 3.7) \times 10^{-12}$ [a,b]	$(2.6 \pm 2.0) \times 10^{-11}$ [a]
C_{1bH}	654.2 [c,d]	654.2 [c,d]	1167 ± 247 [c]
C_{1bD}	1300 ± 230 [c]	820 ± 130 [c]	1760 ± 510 [c]
n_{1b}	0.0001 ± 0.3500	0.0001 ± 1.200	
	$OH + CH_3CH_2OH \rightarrow H_2O + CH_3CH_2O$		
A_{1cH}	$(3.3 \pm 1.7) \times 10^{-12}$ [a]	$(2.1 \pm 6.0) \times 10^{-12}$ [a]	$(2.0 \pm 4.8) \times 10^{-10}$ [a]
A_{1cD}	$(3.3 \pm 1.7) \times 10^{-12}$ [a,b]	$(2.1 \pm 6.0) \times 10^{-12}$ [a,b]	$(3.1 \pm 1.7) \times 10^{-10}$
C_{1cH}	1862 [c,d]	1862 [c,d]	3900 ± 2600
C_{1cD}	2035 ± 104 [c]	4000 ± 6125 [c]	undefined
n_c	2.48 ± 0.49	2.5 ± 2.3	

[a] Units are cm^3 molecule^{-1} s^{-1}. [b] A factors for deuterated reactions are constrained to have the same A factor as for the hydrogenated reactions. [c] Units are Kelvin. [d] Value fixed to that calculated by Sivaramakrishnan et al.[16]

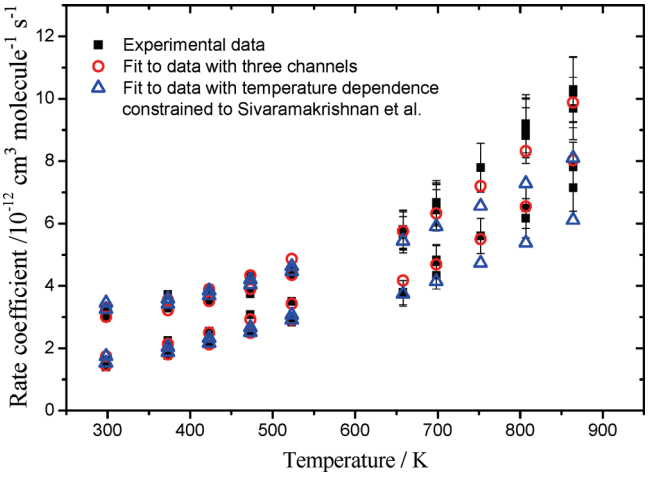

Figure 9. Fits to the complete set of experimental rate coefficients for reaction of OH with various isotopomers, excluding data from the biexponential region: black squares, experimental data points and associated error; red circles, fit to the experimental data using the modified weighted modified Arrhenius parameters of Table 4; blue triangles, fit to the experimental data with the temperature dependence of all channels constrained to the parametrization of Sivaramakrishnan et al.[16] The χ^2 per degree of freedom for the three-channel model is 1.03, increasing to 4.18 for the constrained model.

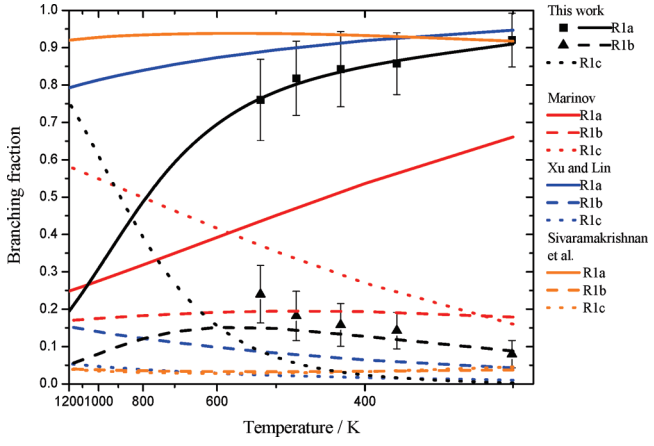

Figure 10. Branching ratios for reaction R1 between 300 and 1200 K. The data points shown are from the lower temperature isotopic studies of this work; the black lines are from fits to the complete data set. Comparisons are shown with branching ratios from the literature where in each case the solid line is the α channel R1a, the dashed line is the β channel R1b, and the dotted line is the OH channel R1c.

reaction R1b. Kinetic traces are once again characterized by single-exponential loss given by eq E8 and shown in Figure 1c.

$$[OH]_t = [OH]_0 \exp(-\kappa' t) \qquad \text{(E8)}$$

where $\kappa' = k_{1.1-1.6}[\text{alcohol}] \times \Gamma + k_{\text{loss}}$ and $\Gamma = (1 - \Phi_{1b}\Phi_{8a})$. $\Phi_{1b}\Phi_{8a}$ represents the yield of OH formed from reactions R1b and R8a but is undetermined in these experiments. If Φ_{8b} is negligible, the returned values of κ', given in Table 3 and Figure 8, represent the rate of OH + ethanol via reactions R1a and R1c only.

For these experiments OH was generated from photolysis of N_2O/H_2O; the presence of water prevented any isotopic substitution of the hydroxyl group but was required to rapidly relax vibrationally excited OH formed from the $O(^1D)$ reactions used to generate OH. Prior to each measurement of a bimolecular rate coefficient for a deuterated species the corresponding rate

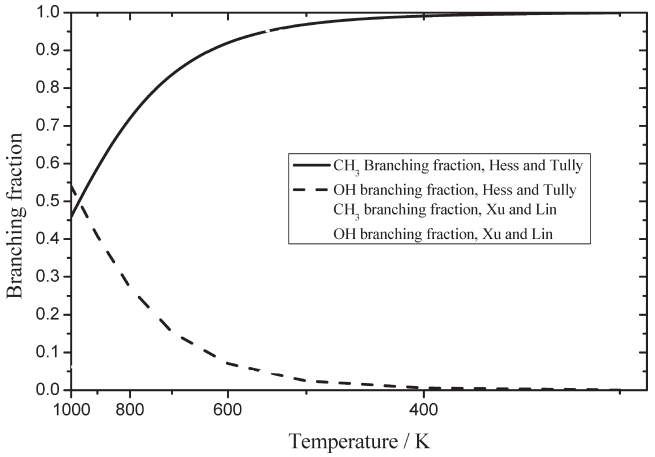

Figure 11. Branching fractions for reaction of OH with methanol: black lines, fits to data of Hess and Tully;[10] gray lines, calculations of Xu and Lin.[17].

coefficient for normal ethanol was measured, and hence, there are three entries for $\kappa_{1.1}$ for each temperature in Table 3 which give a good measure of the reproducibility of the kinetic data. The activation energy for $\kappa_{1.1}$ is 13.2 ± 0.4 kJ mol^{-1}. Our measurements for $\kappa_{1.1}$ are in excellent agreement with the Arrhenius parametrization of the shock tube data of Sivaramakrishnan et al.[16] at the overlapping temperatures, but the data of Sivaramakrishnan display a weaker temperature dependence (E/R = −911 ± 191 K vs −1590 ± 50 K, Figure 4) than this work or Hess and Tully.[6]

Our measurements of $\kappa_{1.1}$ extend those of Hess and Tully[6] and show stronger temperature dependence than would be expected based on extrapolation of the lower temperature (300−500 K) results (Figure 4). Such curvature could arise from strong non-Arrhenius dependence of the α abstraction channel, increased contributions from the hydroxyl abstraction, or a combination of both contributions. Unfortunately, reaction at the hydroxyl group could not be directly investigated as the use of water as an OH precursor caused complete exchange of ROD to ROH.

The measured rate coefficient should be that for channels R1a + R1c as all the CH_2CH_2OH formed in channel R1b is rapidly recycled on the time scale of the experiments to OH. As discussed above, alternative decomposition channels for CH_2CH_2OH have been proposed. Additionally, Dunlop and Tully[15] suggested during a study of 2-propanol + OH that the analogous decomposition of the β-hydroxy radical, $CH_2CHOHCH_3$, has another channel approximately five times slower than the decomposition that forms OH. While the theoretical studies of Senosiain et al.,[35] Cleary et al.,[21] and Xu et al.[36] showed that reaction R8a was the only significant decomposition or isomerization loss process below 650 K, at the very highest temperatures of this study, Xu et al. suggest that an alternative decomposition to form vinyl alcohol + H atom could contribute up to 10% of $HOCH_2CH_2$ loss.[36] If a significant fraction of $HOCH_2CH_2$ was lost without regeneration of OH, then channel R1b (abstraction at the β position) would again start to contribute to OH loss and be evidenced by a KIE. The lack of any significant KIE on deuteration of the β position (e.g., comparing $\kappa_{1.1}$ and $\kappa_{1.2}$ or $\kappa_{1.3}$ and $\kappa_{1.4}$) is consistent with the theoretical calculations of no or only a minor (<20%) loss of $HOCH_2CH_2$ without OH regeneration.[36]

DISCUSSION

Branching Ratios Below 650 K. At low temperatures (300−523 K) isotopic studies have allowed determination of branching ratios from the reaction of OH + C_2H_5OH. Reaction at the hydroxyl channel, Φ_{1c}, is insignificant. Branching ratios between channels Φ_{1a} (α abstraction) and Φ_{1b} (β abstraction) at 300 K are in good agreement with the current values used in the Master Chemical Mechanism and recommended by IUPAC but differ significantly at low temperatures from those recommended by Marinov,[37] although it should be noted that the Marinov model is based on analysis of higher temperature data.

At higher temperatures (550−650 K) decomposition of the $HOCH_2CH_2$ radical formed following β abstraction produces biexponential OH decays. The observation of such decays conflicts with the recent calculations of Sivaramakrishnan et al.,[16] who calculate that both the β and the OH channel are only very minor components of reaction R1 (<4%) up to 1000 K. While Φ_b is relatively poorly determined from our biexponential data, the value of Φ_b at 650 K (0.08 ± 0.14) is not consistent with an extrapolation of the lower temperature isotope data, which would predict Φ_b to be approximately 0.3 at 650 K. The reduction in Φ_b suggests that the hydroxyl abstraction reaction is starting to become significant in this temperature region.

Branching Ratios Determined from Fitting the Complete Set of Exponential Data (298−523 and 658−865 K). Substantial curvature is observed in the the rate coefficients of the overall reaction (300−625 K) and at higher temperatures (658−864 K) for loss via the α and OH channels. The entire kinetic data set can be fitted using a consistent set of parameters for the three channels, either in Arrhenius format (in which case the observed curvature in the rate coefficients is solely associated with variations in the branching ratios) or with modified Arrhenius parameters ($k = AT^n \exp(C/T)$). The returned parameters are shown in Table 4. Floating all parameters in the modified Arrhenius equation for both H and D abstraction provides undefined fits, and hence, the H abstraction barriers were fixed from the calculations of Sivaramakrishnan et al.[16] and it was assumed that the site-specific H/D abstraction rate coefficients have the same A factor. In the high-temperature regime the β channel recycles OH with unit efficiency and this is explicitly included in the data fitting. The returned barriers for the D abstraction sites were consistent with the difference in the zero-point energy, and the resulting fits to the experimental data are shown as the circular points in Figure 9. The fits suggest a substantial contribution from the hydroxyl channel at higher temperatures, and the branching ratios for reaction R1 using the fitted parameters of Table 4 are shown in Figure 10.

Whichever method of fitting is used (Arrhenius, modified Arrhenius, weighted, or nonweighted) the results of the fits at low temperature are in good agreement with the isotopic analysis presented earlier (Figures 9 and 10). Below 523 K, the hydroxyl channel does not contribute significantly to the reaction which is dominated by abstraction from the CH_2 group. Fitting with Arrhenius parameters gives the largest contribution to channel Φ_{1c} (53% at 865 K); Φ_{1c} is slightly lower if modified Arrhenius parameters are used (47%).

Supporting, but, indirect evidence for a significant OH channel comes from a comparison of the OH + ethanol and methanol systems. Hess and Tully[10] studied the reaction of OH with CH_3OH and CD_3OH from 300 to 865 K. Assigning the marked decrease in the isotope effect at 600 K to the onset of abstraction

Table 5. Branching Ratios to the α, β, and OH Channels in Selected Calculations and Modeling Studies at 900 K

	Sivaramakrishnan et al.[16]	Xu and Lin[17]	Dagaut and Togbe[13]	Frassoldati et al.[12]	Norton and Dryer[40]	Marinov[37]	Lin[39]	Saxena and Williams[14]	this work
Φ_{1a}	0.93	0.83	0.77	0.64	0.54	0.30	0.25	0.25	0.39
Φ_{1b}	0.04	0.13	0.17	0.27	0.27	0.18	0.40	0.39	0.10
Φ_{1c}	0.03	0.04	0.06	0.10	0.19	0.53	0.35	0.35	0.51

from the OH site, they estimated that approximately 50% of the total reaction at 865 K occurred via the hydroxyl channel, giving a site-specific rate coefficient of $k_{OH,\ 865K} \approx 3 \times 10^{-12}$ cm^3 molecule^{-1} s^{-1}. The O−H bond strengths in methanol and ethanol are almost identical ($\Delta_r H$ for OH + $CH_3OH \rightarrow CH_3O + H_2O$ and OH + $C_2H_5OH \rightarrow CH_3CH_2O + H_2O$ are −60 and −62 kJ mol^{-1}, respectively[38]), and therefore, one might assume that to a first approximation the rate coefficients for abstraction via the OH channel would be similar. At 865 K a OH site-specific rate coefficient of 3×10^{-12} cm^3 molecule^{-1} s^{-1} would correspond to $\Phi_{1c} = \sim 0.3$ compared to values of 0.47−0.53 determined from our fits to the data.

The OH + CH_3OH kinetic data set of Hess and Tully[10] can be fitted in the same way as we fitted the complete ethanol data set. There is significant curvature in the kinetic data requiring the use of modified Arrhenius parameters ($AT^n \exp(-C/T)$), and the barriers for abstraction from CH_3 and OH were required to be constrained to provide a fit. We used the values calculated by Xu and Lin.[17] Fitting the data gives the following modified Arrhenius parameters: $k_{CH_3} = 4.66 \times 10^{-12}(T/300)^{0.43} \exp(-503/T)$ cm^3 molecule^{-1} s^{-1} and $k_{OH} = 2.48 \times 10^{-13}(T/300)^{4.08} \exp(-1811/T)$ cm^3 molecule^{-1} s^{-1} and branching ratios shown in Figure 11. The calculated branching ratio for abstraction at the OH group at 865 K is 0.64, giving a site-specific rate coefficient of 4.1×10^{-12} cm^3 molecule^{-1} s^{-1}; applying this site-specific rate coefficient to the OH + ethanol reaction gives $\Phi_{1c} = \sim 0.4$ in slightly better agreement with our fits.

In the absence of definitive observation of the products of channel R1c or OD/^{18}OH experiments, it should be noted that an alternative interpretation of the mechanism of reaction can still provide fits to the observed experimental data albeit with higher residuals. Figure 9 compares fits to the data with our modified Arrhenius parameters based on contributions from all three channels (green circles) and a fit based on the α, β, and OH abstractions (blue triangles) from Sivaramakrishnan et al.[16] For the latter fit the $T^n \exp(-C/T)$) dependence of the α and β and OH channels have been constrained to the parameters given by Sivaramakrishnan et al.[16] and the temperature-independent A components have been allowed to float. There is good agreement at lower temperatures including predicted regeneration of OH from the β channel, and above 650 K, the fits lie slightly below the experimental error bars. This constrained model predicts essentially no OH abstraction at all temperatures.

In the Sivaramakrishnan et al. model the observed curvature at higher temperatures arises almost solely from the curvature of the α channel. The high-level ab initio calculations of Sivaramakrishnan et al. suggest that such reactions which have low or submerged barriers with complex hindered internal rotations, possibly further complicated by hydrogen bonding, can exhibit significant curvature as evidenced by their modified Arrhenius parametrization of their transition state calculations: $k_{1a} = 1.19 \times 10^{-19} T^{2.54} \exp(772/T)$ cm^3 molecule^{-1} s^{-1}. The complex structure of the transition state can generate significant temperature dependences in the isotope effect. In the OH/methanol system, Hess and Tully assigned their observed change in isotope effect as being due to a change in mechanism, but alternative explanations are possible.

The quality of the fit of the two-parameter model could be improved by adjusting the parameters of the α and β channels; however, a two-channel model would not predict the decrease in Φ_{1b} observed in the biexponential region between 575 and 650 K. The model would predict that Φ_{1b} continues to monotonically increase, and hence, the total rate coefficient for ethanol removal would be significantly greater than that observed in the studies monitoring OH, a difference which should be readily observable in planned ^{18}OH studies.

Comparison with Branching Ratios Used in Combustion Models. Marinov's[37] analysis of products (acetaldehyde, ethene, and formaldehyde as well as methyl radicals) in jet stirred reactor studies of ethanol oxidation at ∼1070 K (equivalence ratio of unity) shows the importance of the branching ratios of the OH + ethanol reaction on the product distribution. Acetaldehyde is formed from the reactions of CH_3CHOH (70%) and CH_3CH_2O (30%) with molecular oxygen. Fifty five percent of ethene is formed via β abstraction, forming CH_2CH_2OH followed by decomposition, with a further 27% of ethene coming from ethanol dehydration ($C_2H_5OH \rightarrow C_2H_4 + H_2O$). Decomposition of CH_3CH_2O ($CH_3CH_2O \rightarrow HCHO + CH_3$) is the dominant route to formaldehyde production and a major source of methyl radicals. Reactions of other radicals (H, O, CH_3, HO_2) will contribute to production of C_2H_5O isomers, and hence, end-product analysis cannot be used to unambiguously assign product channels of individual reactions.

A number of modeling studies[12−14,37,39] have used temperature-dependent branching ratios for the OH + ethanol reaction. These studies have optimized yields, burning velocities, or ignition delays at temperatures above those of this study, and hence, comparisons with this study should not be too rigorous but nevertheless show important differences. Broadly, the modeling studies split into two groups: those with a low value for k_{1c} and dominance of k_{1a} and, second, those where k_{1b} and k_{1c} play a much more significant role. Table 5 compares the branching ratios of α, β, and OH abstraction from various calculations and models at 900 K.

Branching ratios of reaction R1 play an important role in the subsequent chemistry of ethanol combustion and influence parameters such as flame speeds, etc. Given the uncertainties in high-temperature branching ratios there is a clear need for more definitive experiments under conditions more relevant to combustion. Studies of isotopically labeled OH (either OD or ^{18}OH) would provide a direct measurement of the total rate coefficient and the branching ratio to the β channel. Reliable isotopic studies of the OH channel are likely to be difficult, and direct determination of the ethoxy channel may be a more productive route to follow to quantify the contribution from channel R1c.

SUMMARY

Rate coefficients for the reaction of OH with normal ethanol and several partially deuterated ethanols have been measured as a

function of temperature. The reaction of OH with C_2H_5OH has been studied from 298 to 865 K, extending the temperature range of study. Below 550 K the measured rate coefficients correspond to loss via all possible abstractions, and the results are in excellent agreement with previous work. Above 650 K the measured rate coefficient is for the loss of OH via reaction at the α and OH sites. The rate coefficients are in good agreement with the earlier study of Hess and Tully[6] and agree with the more recent shock tube study of Sivaramakrishnan et al.[16] where the two studies overlap at approximately 860 K. Our measured temperature dependence is stronger than that of Sivaramakrishnan et al.

Branching ratios were determined over the temperature range 300−523 K via isotopic studies; abstraction from the α site (reaction R1a) dominates in good agreement with the current IUPAC evaluation and hence with the value used in the Master Chemical Mechanism to model atmospheric oxidation of ethanol. Reaction at the OH site (reaction R1c) is not significant below 500 K.

Between 550 and 650 K, biexponential OH decays provide further direct evidence of the β abstraction (reaction R1b) in contrast to the calculations of Sivaramakrishnan et al.[16] Φ_{1b} decreases with temperature in this region, suggesting that the hydroxy abstraction channel (reaction R1c) starts to become significant. Fitting our entire set of isotopic data suggests that at 865 K Φ_{1c} ranges from 0.47 to 0.53 depending on our method of fitting. The data can be fitted with a constrained model, based on recent theoretical calculations;[16] however, the quality of the fit is not as good and such a model would not reproduce the observed decrease in Φ_{1b} observed in the biexponential region. More direct studies are required to constrain these branching ratios.

AUTHOR INFORMATION

Corresponding Author

*E-mail: p.w.seakins@leeds.ac.uk.

ACKNOWLEDGMENT

This work was performed with funding from EPSRC including a studentship for S.A.C. under grant GR/T28560/01. We are particularly grateful for discussions with Dr. F. M. Haas, Prof F. L. Dryer, and Dr. S. J. Klippenstein.

REFERENCES

(1) Farrell, A. E.; Plevin, R. J.; Turner, B. T.; Jones, A. D.; O'Hare, M.; Kammen, D. M. *Science* **2006**, *311*, 506.
(2) Olivella, S.; Sole, A. *J. Phys. Chem. A* **2004**, *108*, 11651.
(3) Kuwata, K. T.; Dibble, T. S.; Sliz, E.; Petersen, E. B. *J. Phys. Chem. A* **2007**, *111*, 5032.
(4) Zador, J.; Fernandes, R. X.; Georgievskii, Y.; Meloni, G.; Taatjes, C. A.; Miller, J. A. *Proc. Combust. Inst.* **2009**, *32*, 271.
(5) IUPAC. Evaluated Kinetic Data; IUPAC Subcommittee for Gas Kinetic Data Evaluation, 2007.
(6) Hess, W. P.; Tully, F. P. *Chem. Phys. Lett.* **1988**, *152*, 183.
(7) Wallington, T. J.; Kurylo, M. J. *Int. J. Chem. Kinet.* **1987**, *19*, 1015.
(8) Jimenez, E.; Gilles, M. K.; Ravishankara, A. R. *J. Photochem. Photobiol. a: Chem.* **2003**, *157*, 237.
(9) Dillon, T. J.; Holscher, D.; Sivakumaran, V.; Horowitz, A.; Crowley, J. N. *Phys. Chem. Chem. Phys.* **2005**, *7*, 349.
(10) Hess, W. P.; Tully, F. P. *J. Phys. Chem.* **1989**, *93*, 1944.
(11) Meier, U.; Grotheer, H. H.; Riekert, G.; Just, T. *Chem. Phys. Lett.* **1985**, *115*, 221.
(12) Frassoldati, A.; Cuoci, A.; Faravelli, T.; Ranzi, E. *Combust. Sci. Technol.* **2010**, *182*, 653.
(13) Dagaut, P.; Togbe, C. *Energy Fuels* **2008**, *22*, 3499.
(14) Saxena, P.; Williams, F. A. *Proc. Combust. Inst.* **2007**, *31*, 1149.
(15) Dunlop, J. R.; Tully, F. P. *J. Phys. Chem.* **1993**, *97*, 6457.
(16) Sivaramakrishnan, R.; Su, M.-C.; Michael, J. V.; Klippenstein, S. J.; Harding, L. B.; Ruscic, B. *J. Phys. Chem. A* **2010**, *114*, 9425.
(17) Xu, S.; Lin, M. C. *Proc. Combust. Inst.* **2007**, *31*, 159.
(18) Galano, A.; Alvarez-Idaboy, J. R.; Bravo-Perez, G.; Ruiz-Santoyo, M. E. *Phys. Chem. Chem. Phys.* **2002**, *4*, 4648.
(19) Carr, S. A.; Baeza-Romero, M. T.; Blitz, M. A.; Price, B. J. S.; Seakins, P. W. *Int. J. Chem. Kinet.* **2008**, *40*, 504.
(20) Carr, S. A.; Romero, M. T. B.; Blitz, M.; Pilling, M. J.; Heard, D. E.; Seakins, P. W. *Chem. Phys. Lett.* **2007**, *445*, 108.
(21) Cleary, P. A.; Romero, M. T. B.; Blitz, M. A.; Heard, D. E.; Pilling, M. J.; Seakins, P. W.; Wang, L. *Phys. Chem. Chem. Phys.* **2006**, *8*, 5633.
(22) Aker, P. M.; Sloan, J. J. *J. Chem. Phys.* **1986**, *85*, 1412.
(23) Atkinson, R.; Baulch, D. L.; Cox, R. A.; Crowley, J. N.; Hampson, R. F.; Hynes, R. G.; Jenkin, M. E.; Rossi, M. J.; Troe, J. *Atmos. Chem. Phys.* **2006**, *6*, 3625.
(24) Taylor, S. E.; Goddard, A.; Blitz, M. A.; Cleary, P. A.; Heard, D. E. *Phys. Chem. Chem. Phys.* **2008**, *10*, 422.
(25) Shannon, R. J.; Taylor, S.; Goddard, A.; Blitz, M. A.; Heard, D. E. *Phys. Chem. Chem. Phys.* **2010**, *12*, 13511.
(26) Droege, A. T.; Tully, F. P. *J. Phys. Chem.* **1986**, *90*, 1949.
(27) Droege, A. T.; Tully, F. P. *J. Phys. Chem.* **1986**, *90*, 5937.
(28) Tully, F. P.; Droege, A. T.; Koszykowski, M. L.; Melius, C. F. *J. Phys. Chem.* **1986**, *90*, 691.
(29) Tully, F. P.; Goldsmith, J. E. M. *Chem. Phys. Lett.* **1985**, *116*, 345.
(30) Hu, W. P.; Rossi, I.; Corchado, J. C.; Truhlar, D. G. *J. Phys. Chem. A* **1997**, *101*, 6911.
(31) Saunders, S. M.; Jenkin, M. E.; Derwent, R. G.; Pilling, M. J. *Atmos. Chem. Phys.* **2003**, *3*, 161.
(32) Rickard, A. R.; Jenkin, M. E.; Pilling, M. J., 2010. http://mcm.leeds.ac.uk/MCM/.
(33) Diau, E. W. G.; Lee, Y. P. *J. Chem. Phys.* **1992**, *96*, 377.
(34) Fulle, D.; Hamann, H. F.; Hippler, H.; Jansch, C. P. *Ber. Bunsen-Ges. Phys. Chem. Chem. Phys.* **1997**, *101*, 1433.
(35) Senosiain, J. P.; Klippenstein, S. J.; Miller, J. A. *J. Phys. Chem. A* **2006**, *110*, 6960.
(36) Xu, Z. F.; Xu, K.; Lin, M. C. *Chemphyschem* **2009**, *10*, 972.
(37) Marinov, N. M. *Int. J. Chem. Kinet.* **1999**, *31*, 183.
(38) Sander, S. P.; Friedl, R. R.; Golden, D. M.; Kurylo, M. J.; Huie, R. E.; Orkin, V. L.; Moortgat, G. K.; Ravishankara, A. R.; Kolb, C. E.; Molina, M. J.; Finlayson-Pitts, B. J. *Chemical Kinetics and Photochemical Data for Use in Atmospheric Studies*; Jet Propulsion Laboratory: Pasadena, CA, 2003.
(39) Lin, J. Experimental and Numerical Studies of Ethanol Chemical Kinetics. Ph.D. Thesis, Princeton, 2004.
(40) Norton, T. S.; Dryer, F. L. *Int. J. Chem. Kinet.* **1992**, *24*, 319.